*Geophys. J. R. astr. Soc.* (1970), **21**, 119–129.

# Enhancement of Teleseismic Body Phases with a Polarization Filter

**James F. Montalbetti and Ernest R. Kanasewich**

(Received 1970 March 9)

*Summary*

A time domain polarization filter, originally proposed by Flinn, has been modified and is used to increase the signal to noise ratio of teleseismic body phases. Both the rectilinearity and direction of particle motion is obtained from the co-variance matrix for three components of ground motion over a small time interval. The estimate of rectilinearity is found by diagonalizing the matrix and forming a function that involves the ratio of the largest and intermediate principle axes of the matrix. The direction of polarization is found from the eigenvector of the largest principle axis. A set of time-varying operators are then obtained which act as a point by point gain control to modulate the digital seismic records. This non-linear filter is useful for enhancing *P*, *pP*, *sP*, *PP*, *S* and other compressional or shear phases. When applied to an array of three-component stations it appears to be possible to identify multiple events in the source function of some earthquakes.

## 1. Introduction

As any seismograph record is always noise contaminated, the detection and interpretation of seismic events requires knowledge of the characteristics of both signal and noise. Elastic body waves, which may be generally separated into *P* (compressional) and *S* (shear) phases, can be considered as non-dispersive group arrivals with maximum power in the 0·3 to 10-second period range. Surface Rayleigh and Love waves may be described as dispersive group arrivals with maximum power in the 2-to 100-s period range for earthquakes of moderate magnitude, the observable periods extending up to 57 min for larger teleseismic events.

Superimposed on these signals is microseismic background noise as well as signal generated noise. Signal generated noise is the result of multiple reflections and refractions of *P* and *S* body waves at crustal interfaces and inhomogeneities and local conversion of body waves to surface waves; this type of noise originates primarily under the recording station. Microseismic noise, which is considered to consist mainly of fundamental and higher mode Rayleigh waves, has been shown to exhibit a sharp peak in the 5-to 8-s period range (Brune & Oliver 1959). As a result of this sharp peak in the microseismic noise spectrum, frequency bandpass filtering is often employed to improve the signal to noise ratio. Although this type of filtering is very effective in removing microseismic background from both long and short period data, it often cannot distinguish between signal and signal generated noise. Difficulty may still arise in the attempted identification of phases whose frequency characteristics are similar.

A further property of seismic events which may be used for the enhancement of recorded data is that of signal polarization. Both compressional and shear waves exhibit a high degree of linear polarization. Particle motion coincides with the azimuth of propagation of energy for compressional ($P$) phases and is perpendicular to the azimuth of propagation for the transverse ($S$) phases. Surface waves of the Rayleigh type are generally elliptically polarized in the vertical–radial plane, the fundamental modes displaying retrograde particle motion and the higher modes prograde or retrograde ellipticity. Surface Love waves are also found to be rectilinearly polarized, but in a horizontal plane orthogonal to the direction of wave propagation. Since most microseismic background is of the Rayleigh type, it will exhibit elliptical polarization, but with little preferred directionality. Signal generated noise may also be polarized, but again the direction of polarization is random in nature. By using these various characteristics of polarized particle trajectories, filters may be designed which preserve motion if it satisfies specified conditions of polarization in a particular direction, and which attenuate motion that does not satisfy the desired criteria.

Considering these patterns of particle motion, various workers have designed polarization filters for the enhancement of seismic data. Shimshoni & Smith (1964) suggest that the time averaged cross product of vertical and radial components of ground motion may be used as a measure of rectilinearity. The computed cross product is multiplied by the original signal so that a function of ground motion which enhances rectilinearly polarized signal is obtained. Another process described by the same workers computes the parameters of an equivalent ellipse at each instant in time, from the Fourier Components of the vertical and radial motions. Eccentricity, major axis, and angle of inclination of the ellipse from the vertical are displayed for the frequency at which maximum power is arriving and used to provide criterion for the identification of $P$ and $SV$ type motion.

Various workers have applied polarization filtering techniques to recorded seismic data for improvement of the signal to noise ratio. Lewis & Meyer (1968) apply a phase filter of the REMODE type as described by Archambeau & Flinn (1965) and originally developed by Mims & Sax (1965) with subsequent work by Griffin (1966a, b) to data recorded during the Early Rise experiment in the summer of 1966. Archambeau, Flinn & Lambert (1969) used the same filter to study multiple $P$ phases from NTS explosions. In another application, Basham & Ellis (1969) use a REMODE filter designated as a $P$-Detection ($P$–$D$) filter to process $P$-wave codes of numerous seismic events recorded in western Alberta. The polarization filter applied to 25 s of record following the $P$ onset aids in identification of numerous compressional wave arrivals including $P$, $p^P$ and $sP$. $P_c P$ and $PKP$ phases for events at appropriate epicentral distances are also detected.

Polarization filters can be more useful than frequency filters for enhancement of signal to noise ratio particularly when the signal and noise have similar spectral characteristics. These types of filters however, are time-varying non-linear processors and their applications require more computer time than for example a digital frequency filter whose response does not change with time, and which may be applied recursively in the time domain.

## 2. Design of the filter

The design of the polarization filter used in this paper is a variation on one described by Flinn (1965) in which both rectilinearity and direction of particle motion is considered. In order to obtain measures of these two quantities, the co-variance matrix for a set of $N$ points taken over each of the three orthogonal components of ground motion, $R$ (Radial), $T$ (Transverse) and $Z$ (Vertical) is computed. For a three-component digital seismogram then, a specified time window of length $N\Delta t$, where $\Delta t$ is the sampling interval, is thus considered. To determine the covariance matrix for this set of observations, the means, variances and covariances must be calculated for the three variables $R$, $T$ and $Z$.

We define the mean or expected value of $N$ observations of the random variable $X_{1i}$ $(i = 1, 2, \ldots, N)$ as

$$\mu_1 = \frac{1}{N} \sum_{i=1}^{N} X_{1_i} = E(X_1). \tag{1}$$

The co-variance between $N$ observations of two variables $X_1$ and $X_2$ is given by

$$\mathrm{Cov}[X_1, X_2] = \frac{1}{N} \sum_{i=1}^{N} (X_{1_i} - \mu_1)(X_{2_i} - \mu_2) \tag{2}$$

where $\mu_1$ and $\mu_2$ are computed as in equation (1). It is evident that

$$\mathrm{Cov}[X_1, X_2] = \mathrm{Cov}[X_2, X_1].$$

The quantity $\mathrm{Cov}[X_1, X_1]$ is defined as the autoco-variance, or simply the variance of $X_1$. The matrix with $\mathrm{Cov}[X_r, X_s]$ in its $r$th row and $s$th column $(r, s = 1, 2, \ldots, n)$ is the co-variance matrix for the set of $n$ random variables $X_j$, $j = 1, 2, \ldots, n$. If $\bar{X}$ is the vector of the random variables and $\bar{\mu}$ the vector of means for each of these variables, the co-variance matrix $V$ is defined by (Jenkins & Watts, 1968, Chapter 3)

$$V = E[(\bar{X} - \bar{\mu})(\bar{X} - \bar{\mu})^t]. \tag{3}$$

The superscript $t$ indicates the column transpose of the vector. For our case of three variables $R$, $T$ and $Z$ considered over the time window $N\Delta t$, equation (3) is represented by

$$V = \begin{pmatrix} \mathrm{Var}[R] & \mathrm{Cov}[R, T] & \mathrm{Cov}[R, Z] \\ \mathrm{Cov}[R, T] & \mathrm{Var}[T] & \mathrm{Cov}[T, Z] \\ \mathrm{Cov}[R, Z] & \mathrm{Cov}[T, Z] & \mathrm{Var}[Z] \end{pmatrix} \tag{4}$$

where the co-variances and variances are defined in equation (2).

If the co-variance matrix given by equation (4) is diagonalized, an estimate of the rectilinearity of particle motion trajectory over the specified time window can be obtained from the ratio of the principal axes of this matrix. The direction of polarization may be measured by considering the eigenvector of the largest principal axis. If $\lambda_1$ is the largest eigenvalue and $\lambda_2$ the next largest eigenvalue of the co-variance matrix, then a function of the form

$$F(\lambda_1, \lambda_2) = 1 - \left(\frac{\lambda_2}{\lambda_1}\right)^n \tag{5}$$

would be close to unity when rectilinearity is high ($\lambda_1 \gg \lambda_2$) and close to zero when the two principal axes approach one another in magnitude (low rectilinearity). The direction of polarization can be determined by considering the components of the eigenvector associated with the largest eigenvalue with respect to the co-ordinate directions $R$, $T$, and $Z$.

To illustrate this, Figs 1(a)–(d) show some computations applied to sets of data in two dimensions. These points were computed for an ellipse and then perturbed by the addition of random noise. In Figs 1(b) and (d), the data points were generated from a 45° rotation of the original ellipses determined for Figs 1(a) and (b) respectively. The computed co-variance matrix, correlation coefficient $\rho$, $F(\lambda_1, \lambda_2)$ for

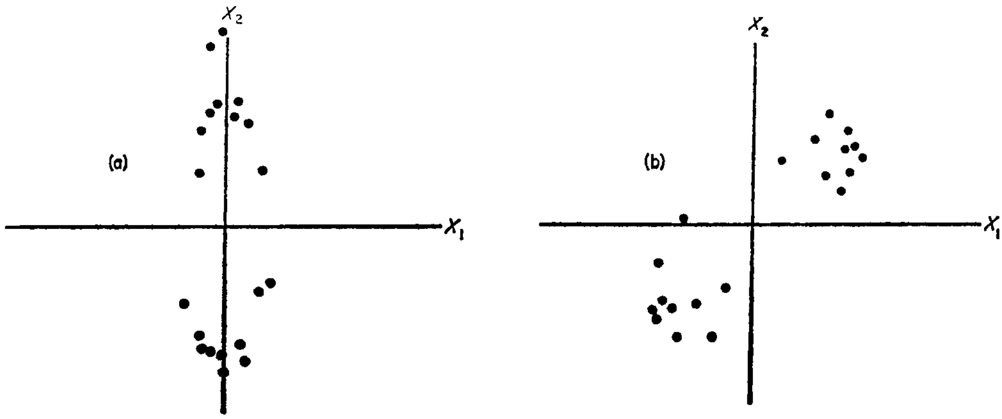


$$V = \begin{bmatrix} 1\cdot317 & -0\cdot237 \\ 0\cdot237 & 26\cdot510 \end{bmatrix}$$

$\rho = 0\cdot040$

$F(\lambda_1, \lambda_2) = 0\cdot950$

$\bar{E} = (-0\cdot009, 0\cdot999)$

$$V = \begin{bmatrix} 13\cdot775 & 11\cdot756 \\ 11\cdot756 & 12\cdot519 \end{bmatrix}$$

$\rho = 0\cdot895$

$F(\lambda_1, \lambda_2) = 0\cdot945$

$\bar{E} = (0\cdot726, 0\cdot689)$

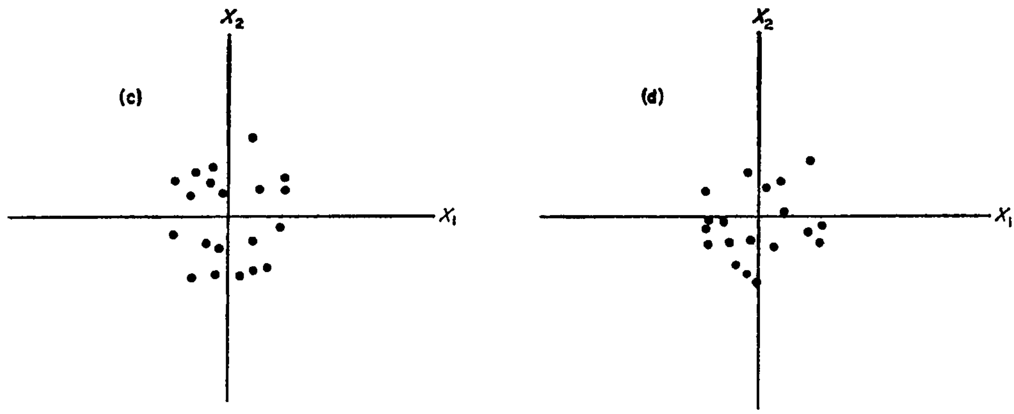


$$V = \begin{bmatrix} 2\cdot416 & 0\cdot221 \\ 0\cdot221 & 3\cdot426 \end{bmatrix}$$

$\rho = 0\cdot077$

$F(\lambda_1, \lambda_2) = 0\cdot318$

$\bar{E} = (0\cdot205, 0\cdot979)$

$$V = \begin{bmatrix} 2\cdot803 & 0\cdot420 \\ 0\cdot420 & 3\cdot085 \end{bmatrix}$$

$\rho = 0\cdot143$

$F(\lambda_1, \lambda_2) = 0\cdot262$

$\bar{E} = (0\cdot584, 0\cdot812)$

FIG. 1. Examples of the co-variance matrix, correlation coefficient, $\rho$, the rectilinearity function $F(\lambda_1, \lambda_2)$ for $n = 1$, and the eigenvector, $E$, of the principal axis for sets of 20 points in two dimensions.

$n = 1$, and the eigenvector of the principal axis, $\bar{E}$, are shown for each case. The correlation coefficient is determined from the usual definition (Jenkins & Watts 1968, Chapter 3)

$$\rho_{12}^2 = \frac{(\mathrm{Cov}[X_1, X_2])^2}{\mathrm{Var}[X_1]\,\mathrm{Var}[X_2]}. \tag{6}$$

Comparing Figs 1(a) and (b) we see that in the first case $\mathrm{Cov}[X_1, X_2]$ is small with respect to the variance terms on the main diagonal, and the eigenvector $\bar{E}$ indicates a preferred direction along the $X_2$-axis. In the second case, Fig. 1(b), $\mathrm{Cov}[X_1, X_2]$ is larger and $\bar{E} = (0{\cdot}726, 0{\cdot}689)$ shows no preferred direction along either the $X_1$ or $X_2$ co-ordinate axis. In both instances $F(\lambda_1, \lambda_2)$, the rectilinearity function, is approximately the same. Similar properties of the covariance matrix and the eigenvector $\bar{E}$ are indicated by Figs 1(c) and (d), but here the rectilinearity, $F(\lambda_1, \lambda_2)$, is low in both cases. We see then that when the off-diagonal terms of the co-variance matrix are significant, the diagonalization will introduce a rotation. After rotation, the orientation in space of the principal axis of the co-variance matrix will be given by the components of its eigenvector relative to the original co-ordinate system. $F(\lambda_1, \lambda_2)$ will give an estimate of the degree of polarization along the major axis. In each of Figs 1(a)–(d), the data points could be considered as representing particle motion trajectory over a specified time in one of the orthogonal planes of the $R$, $T$, $Z$ co-ordinate system.

Suppose now that in the matrix of equation (4) the co-variance terms are small with respect to those on the main diagonal, on which, $\mathrm{Var}[R] > \mathrm{Var}[T] > \mathrm{Var}[Z]$. The lengths of the two principal axes would thus correspond very closely to $\mathrm{Var}[R]$ and $\mathrm{Var}[T]$, and the eigenvector associated with the major axis, $\mathrm{Var}[r]$, would have its largest component in the $R$ co-ordinate direction. If $\mathrm{Var}[R] \gg \mathrm{Var}[T]$, then $F(\lambda_1, \lambda_2)$ in equation (5) would be close to unity and we would have high rectilinearity in the $R$ direction. If $\mathrm{Var}[R] \sim \mathrm{Var}[T]$, then the direction of polarization would still be predominantly along the $R$ co-ordinate axis, but the rectilinearity would be low. If the off-diagonal terms of the matrix were significant, the diagonalization would introduce a rotation, and the orientation in space of the major axis would be given by the components of its eigenvector relative to the original $R$, $T$, $Z$ co-ordinate system. By combining $F(\lambda_1, \lambda_2)$ and the appropriate eigenvector, we see that measures of rectilinearity and directionality can be obtained. Determination of a suitable filter function is then possible.

Applying this analysis to three-component digital seismograms, the co-variance matrix is computed for a specified time window of length $N\Delta t$ centred about $t_o$, where $t_o$ is allowed to range over the entire record length of interest. Eigenvalues and the corresponding eigenvectors of this matrix are then determined. The measure of rectilinearity for the time $t_o$ is given by

$$RL(t_o) = [F(\lambda_1, \lambda_2)]^J \tag{7}$$

where $F(\lambda_1, \lambda_2)$ is defined in equation (5). If we represent the eigenvector of the principal axis with respect to the $R$, $T$, $Z$ co-ordinate system by $\bar{E} = (e_1, e_2, e_3)$ then the direction functions at time $t_o$ are given by

$$D_i(t_o) = (e_i)^K \tag{8}$$

$$i = R, T, Z \equiv 1, 2, 3.$$

Since the eigenvector is normalized ($|E| = 1$), we see that for each of these functions $D_i$

$$0 < D_i < 1.$$

The exponents $J$, $K$ and $n$ (equation (5)) are determined empirically. Once these functions are computed, the window is moved down the record one sample interval and the calculations are repeated.

Weighting functions of this form are used by Flinn (1965) as point by point gain controls and applied to the appropriate component of ground motion. In the course of the present study, it was found that an additional computation was advantageous. When the end of the desired record is reached, the quantities defined by equations (7) and (8) are then averaged over a window equal to about half the original window length. This has the effect of 'smoothing' these operators so that contributions due to any anomolous spikes are subdued. If this time window consists of $M$ points, the gain functions are given by

$$\left.\begin{aligned} RL^*(t_o) &= \frac{1}{M}\sum_{\tau=-L}^{L} R(t_o+\tau) \\ D_i^*(t_o) &= \frac{1}{M}\sum_{\tau=-L}^{L} D_i(t_o+\tau),\ i = R, T, Z \\ L &= \frac{M-1}{2}. \end{aligned}\right\} \tag{9}$$

These operators are then used as a point by point gain control to modulate the rotated records so that at any time $t$, the filtered seismograms are given by

$$\left.\begin{aligned} R_f(t) &= R(t).RL^*(t).D_R^*(t) \\ T_f(t) &= R(t).RL^*(t).D_T^*(t) \\ Z_f(t) &= Z(t).RL^*(t).D_Z^*(t) \end{aligned}\right\} \tag{10}$$

In most cases, the data were band-pass filtered with a zero phase shift digital filter before rotation so that the spectral content of the record was restricted. The window length could be specified so as to be consistent with one or two cycles of the dominant period. Values of $J$ and $K$ which appeared quite adequate were 1 and 2 respectively. For rectilinearity, $n = 0{\cdot}5$ or 1 was used.

A Fortran IV program has been written for application of this polarization filter to three component digital seismograms, using an IBM 360/67 computer. Various events were recorded at the University of Alberta's Edmonton, Geophysical Observatory and at two field stations operated 5 and 10 km for the observatory using a broadband digital recording system described by Burke *et al.* (1970). The three data channels (vertical, east–west horizontal and north–south horizontal) were first bandpass filtered using a recursive zero phase shift digital filter and then rotated into an $R$–$T$–$Z$ co-ordinate system so that the radial direction corresponded to the computed great circle azimuth from source to receiver and the transverse component was orthogonal to this. The program is arranged so that window length for both the co-variance matrix (equation (4)) and the smoothing process (equation (9)), starting point of calculations, and the exponents $J$, $K$ and $n$ can be specified as input data.

## 3. Interpretation of processed data

Fig. 2 shows an event processed by this method. The earthquake, of magnitude 5·9, occurred in the Philippines on 1969, January 30, at a depth of 70 kilometers. The first three traces represent the vertical, radial, and horizontal components of ground motion after bandpass filtering from 0·3–4 Hz and rotation. Trace 4–7 are the filter functions as given by equations (9). The last three represent the records after applying these operators as in equation (10). The filter functions and the processed records are displayed from the point in time where calculations began. We see a good separation of events labeled $P_1$, $P_2$ and $P_3$ in the $P$, $PP$, and $PPP$ codas of the processed seismogram. The good correlation of these events with their respective $pP$ times suggests a multiplicity of sources at the same location rather

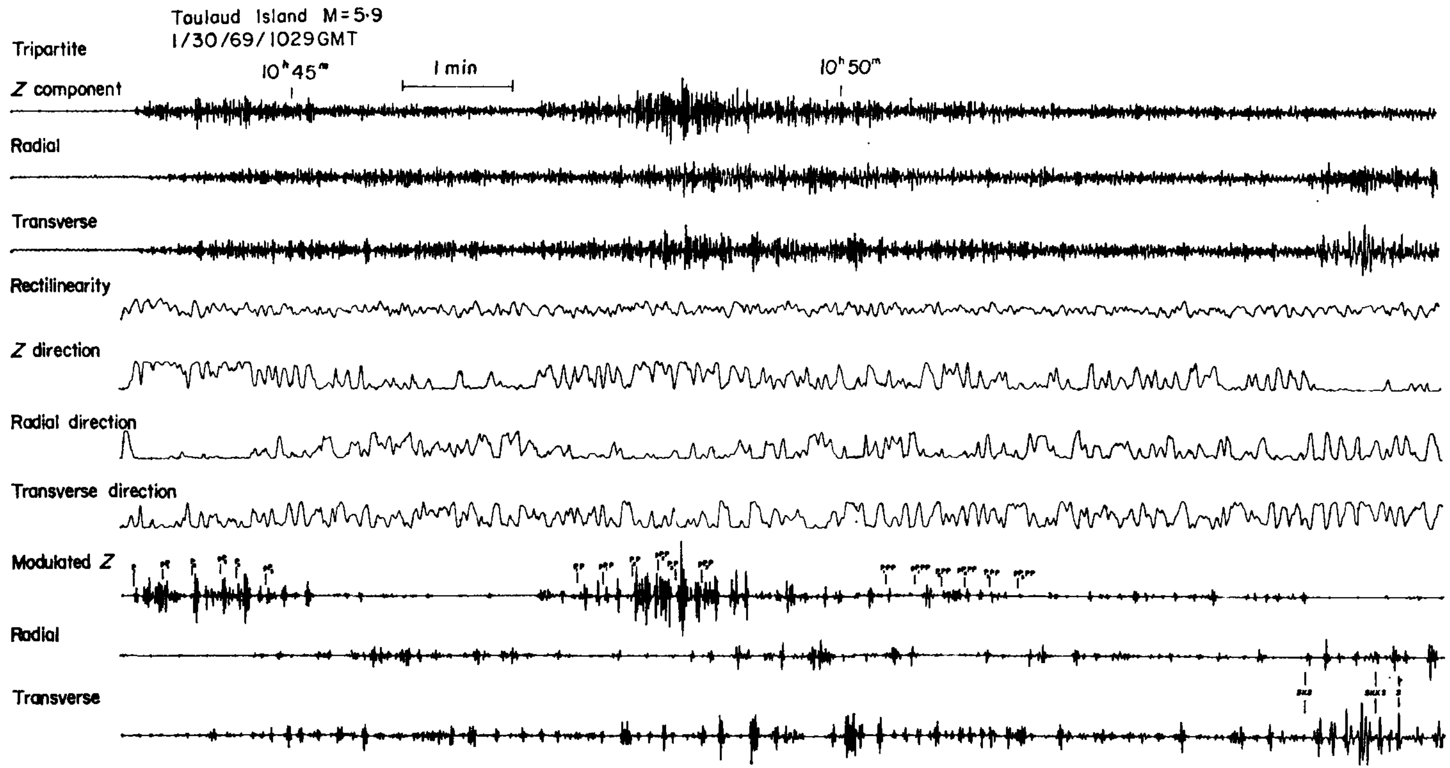


FIG. 2. Example of a magnitude 5·9 earthquake which occurred in the Philippines at 10 h 29 m 40·4 s U.T. on 1969 January 30, processed by the polarization filter with $J = 1$, $K = L = M = 2$, $n = \frac{1}{2}$. Universal time is indicated along the top of the figure. The epicentral distance was 103° and the depth was 70 km. The first three traces are the vertical, radial and transverse components of ground motion respectively; the next four represent the computed filter operators; the last three are the filtered seismograms. The data were bandpass filtered 0·3 to 4 Hz with a zero phase shift operator before the operation shown here.

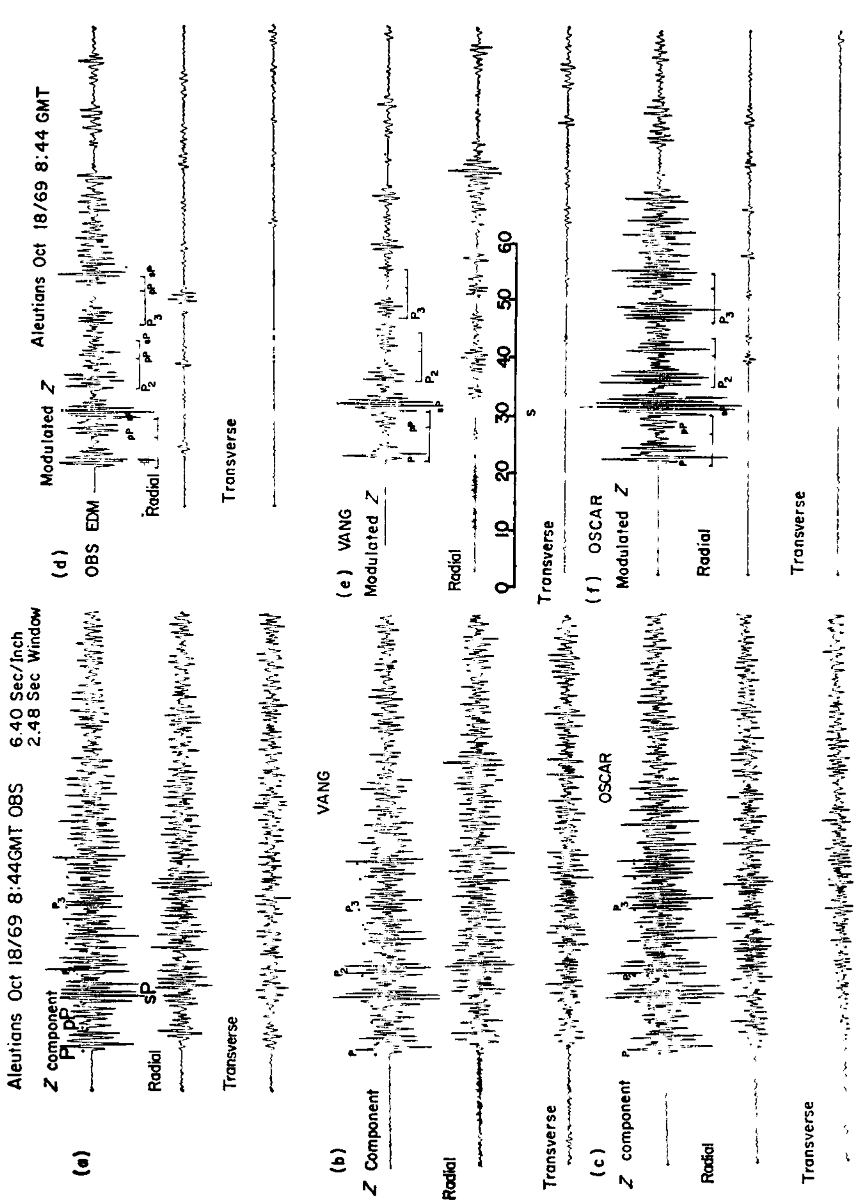


FIG. 3. (a), (b) and (c) are unfiltered three-component recordings at three locations of an earthquake in the Aleutians at 08 h 44 m U.T. 1969, October 18. (d), (e) and (f) show the same recording after filtering with a time domain polarization filter. The magnitude was 5·6 and the depth of focus was 24 km.

than a single release of energy. Attenuation of the radial and transverse traces, especially during the *P* and *PP* events, illustrates how the filter enhances motion which exhibits a preferred direction of polarization, in this case, the *Z* direction. We note also the increase in signal on the two horizontal components and a corresponding decrease in the vertical trace at the begininng of the *SKS–SKKS–S* group of waves which has been identified using predicted times from the Jeffreys–Bullen travel-time curves. This is to be expected since little signal should be present on the vertical component of ground motion when shear (*S*) waves are predominant.

A comparison of filtered and unfiltered records from three recording stations (observatory Edmonton, Vang and Oscar, 5 km apart in a north–south line) for an event which occurred in the Aleutians on 1969, October 18, is shown in Fig. 3. The *CGS* depth determination of 24 km was used to obtain a *P–pP* time for this earthquake and is shown on the *z* components for each record. Enhancement of the *pP* and *sP* arrivals is evident on each of the filtered seismograms (Fig. 3(d), (e) and (f)).

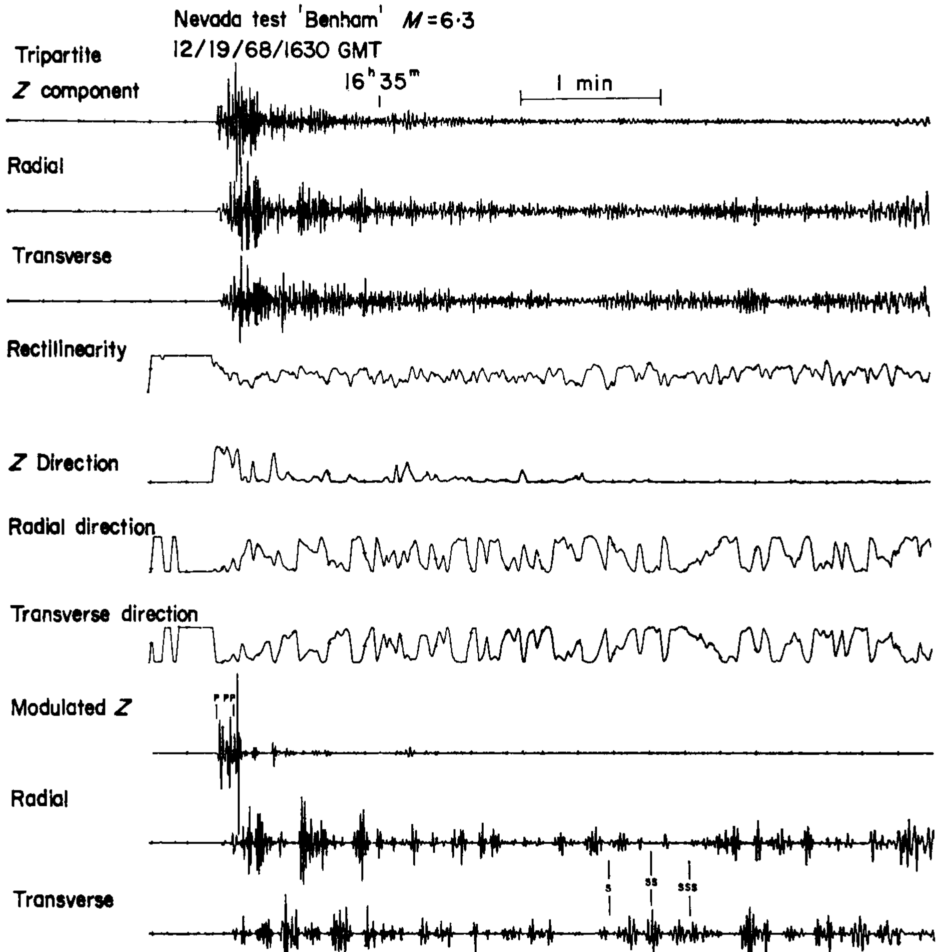


FIG. 4. The nuclear explosion ' Benham ' detonated in Nevada at 16h 30m U.T. on 1968, December 19, as recorded at the Edmonton Observatory. The lower three traces show the event after processing by a polarization filter with the same parameters as in Fig. 2. The event was of magnitude 6·3 and was recorded at $\Delta = 16°$.

The $sP$–$P$ travel time was calculated approximately from a relation based on ray theory:

$$sP-P = h\left\{\frac{1}{\alpha\cos\theta} + \frac{1}{\beta\cos\psi} - \frac{dT}{d\Delta}(\tan\psi + \tan\theta)\right\} \quad (1)$$

in which $dT/d\Delta$ is obtained from a travel-time graph of $P$ arrivals versus epicentral distance, $\Delta$; $\alpha$ and $\beta$ are the average compressional and shear velocities from the focus to the surface and were taken to be 7·6 and 4·4 km $s^{-1}$ respectively; $h$ is the depth of focus; $\sin\theta = \alpha.dT/d\Delta$ and $\sin\psi = (\sin\theta)\beta/\alpha$. The $pP$–$P$ is found in a similar manner if we let $\theta = \psi$ and $\alpha = \beta$ in the equation above. The observed times for $pP$ and $sP$ relative to the $P$ phase is 5·5 and 8·2 seconds and compared to 5·3 and 7·8 seconds calculated on the basis of the *CGS* depth calculation. Events $P_2$ and $P_3$ may be interpreted as earthquakes in the same vicinity and at about the same depth which were triggered by the initial $P$ phase. All three stations show the $P$, $P_2$ and $P_3$ events together with their $pP$ and $sP$ phases reflected from the surface near the event.

Several nuclear shots have been processed by the polarization filter and an example, codenamed Benham, recorded at the Edmonton observatory, is shown in Fig. 4. In this example, as in all others, the processed records show a very simple *P* coda, as would be expected from an explosive source. However, there is a high level of activity exhibited on the transverse and radial records near the beginning of the event which is difficult to account for. The shear phases (*S*, *SS* and *SSS*) are present only on the horizontal components but the bandpass used for recording them was set too high for maximum enhancement. An array of stations is generally essential before it is possible to interpret the converted phases which follow the initial *P* and *S* waves.

## Conclusion

The polarization filter is useful in processing teleseismic data because it tends to enhance phases with well-defined properties. Events may be interpreted and correlated over an array with greater confidence. The modified filter has gain parameters which vary slowly with time so that the signal character is not distorted severely as it is in REMODE type filters. The processed records have been found to be particularly useful when determining the depth of focus. On many earthquakes there appear to be several aftershocks which follow only seconds after the initial event. These aftershocks occur in the same locality and at about the same depth as the initial event which probably serves to trigger the multiple sequence in the source region.

*Division of Geophysics,*
*Department of Physics,*
*University of Alberta,*
*Edmonton, Canada.*

## References

Archambeau, C. B., & Flinn, E. A., 1965. Automated analysis of seismic radiations for source characteristics, *Proc. I.E.E.E.*, **53**, 1876.

Archambeau, C. B., Flinn, E. A. & Lambert, D. G., 1969. Fine structure of the upper mantle, *J. geophys. Res.*, **74**, 5825.

Basham, P. W. & Ellis, R. M., 1969. The composition of *P* codas using magnetic tape seismograms, *Bull. seism. Soc. Am.*, **59**, 473.

Brune, J. N. & Oliver, J., 1959. The seismic noise of the earth's surface, *Bull. seism. Soc. Am.*, **49,** 349.

Burke, M. D., Kanasewich, E. R., Malinsky, J. D. & Montalbetti, J. F., 1970. A wide-band seismograph system, *Bull. seism. Soc. Am.* (in press).

Flinn, E. A., 1965. Signal analysis using rectilinearity and direction of particle motion, *Proc. I.E.E.E.*, **53,** 1874.

Griffin, J. N., 1966a. Application and development of polarization (REMODE) filters: Seismic Data Laboratory Report 141, Teledyne Inc., Alexandria, Va. (AD-630-515)*.

Griffin, J. N., 1966b. REMODE signal/noise tests in polarized noise: Seismic Data Laboratory Report 162, Teledyne, Inc., Alexandria, Va. (AD–800–039).

Jenkins, G. M. & Watts, D. G., 1968. *Spectral analysis and its application*, San Francisco: Holden-Day Co.

Lewis, B. T. R. & Meyer, R. P., 1968. A seismic investigation of the upper mantle to the west of Lake Superior, *Bull. seism. Soc. Am.*, **58,** 565.

Mims, C. H. & Sax, R. L., 1965. Rectilinear motion direction (REMODE): Seismic Data Laboratory Report 118, Teledyne, Inc., Alexandria, Va. (AD–460–631).

Shimshoni, M. & Smith, S. W., 1964. Seismic signal enhancement with three-component detectors, *Geophysics*, **29,** 664.

* AD numbers are the document identification codes used by the Federal Clearinghouse for Scientific and Technical Information, Springfield, Virginia, USA, from which these reports are available for a nominal charge.